Journal of Engineering and Applied Sciences 12 (Special Issue 4): 6675-6683, 2017
ISSN: 1816-949X

Soft Switching Technique of a Secondary Resonant Buck Converter

[1]Kwang-Seok Song, [1]Gwang-Cheol Song, [1]Jung-Hwan Lee, [2]Seong-Mi Park and [1]Sung-Jun Park
[1]Department of Electrical Engineering, Chonnam University, 61186 Gwangju, Korea
[2]Department of Electrical Engineering, Korea Lift College, 50141 Gyeongnam, Korea

Abstract: The development of high efficiency electric light bulbs and high efficiency power converters are drawing high interests in order to realize high efficiency lighting systems. Particularly, high efficiency power converters are showing the trend of being embodied through the reduction of switching losses. Representative methods for reducing switching losses are classified into 2 general categories: reduction of excessive switching losses by soft switching topology and reduction of switch conduction losses by the topology that can decrease the number of conduction switch elements. Particularly, an LED equivalent circuit is expressed with a capacitance of constant capacity and a zener diode that has the characteristics of resistance and threshold voltage. Accordingly, since LED load is different from conventional loads, the embodiment of a high efficiency power converter for operating LED demands a DC/DC topology that is suitable for the characteristics of LED load. This research proposes a new high efficiency DC/DC converter topology for LED street-lamps. The proposed DC/DC converter employed secondary resonance to achieve soft switching when the switch is turned on/off. In addition, it was possible to reduce switch conduction losses by configuring the resonance circuit with a current loop that has a single semiconductor element. Simulation experiments using Psim were carried out to verify the performance of the DC/DC converter and the result confirmed its excellence.

Key words: Secondary resonance, soft switching, DC/DC converter, LED, street lamps, resistance

INTRODUCTION

LED lighting industry is emerging as a national strategic parts and material industry as an alternative industry for energy saving, to cope with energy crisis. Incandescent light bulbs and fluorescent light bulbs which are the representative products of conventional lighting are showing limitations to technical improvement. Meanwhile, it is a current trend that developed countries ban the sale of incandescent light bulbs. For such reasons there is a growing demand for a new high efficiency light source.

High efficiency LED, a representative DC light source developed recently has the merits of low power consumption, long life and rapid turn-on/off. Accordingly, active researches are going on to improve the efficiency of high output LED in order to use it for common lighting. An LED System for lightning consists of a light source utilizing LED and an operation circuit for operating the LED source (Shin *et al*., 2010; Choi *et al*., 2009). LED is similar to diode in characteristics and at voltages higher than threshold voltage, it shows the characteristic of rapid increase in current change according to voltage change. Therefore, DC power suppliers for LED operation prefers the constant-current method to the constant-voltage method used for conventional SMPS. Constant-current LED drivers can be classified into 2 types according to the types of circuit: the AC voltage to DC current type and the DC voltage to DC current type (Park *et al*., 2009; Choi *et al*., 2009).

The AC voltage to DC current type is widely used as an operation circuit for common LED lighting systems. Whereas the DC voltage to DC current system is widely used as an operation system for the street-lamps which use DC power as input power such as the street-lamps utilizing sunlight or wind power. Demand for such drivers is anticipated to increase rapidly in the future when a DC distribution system is applied. In order to improve the efficiency of the LED operation circuit for lighting, this research proposes a new dual resonant buck-type DC/DC converter topology that enables soft switching when the switch is turned on/off. In addition, the excellent performance of the proposed DC/DC converter was verified by simulation experiments using PSIM.

MATERIALS AND METHODS

LED driver: LED drivers using DC input power can be classified into 2 types as shown in Fig. 1, the DC voltage to DC voltage type and the DC voltage to DC current type (Kang, 2013).

The DC voltage to DC voltage type, like conventional SMPS, uses DC power as input power to generate the final output of DC power and it is seldom used as an LED

Corresponding Author: Kwang-Seok Song, National Institute of Standards and Technology, 80305 Boulder, USA

operation circuit. In contrast, the DC voltage to DC current type uses DC voltage as input power to supply constant DC current to terminal LED and it is widely used as an operation system for the lighting equipment that use DC power as input power such as the lighting equipment utilizing sunlight or wind power.

For the designing of an LED module, it is necessary first to determine the number of LED operations. Once the light flux of an LED and the number of LEDs in series have been determined by selecting an LED package, the light flux of an array is determined. Then, the structure of LED array has to be determined considering the light flux of an array and the light flux demanded. LED array can be configured in either series, parallel or series-parallel structure. And the numbers of LEDs in series and parallel are determined according to the size of the light source and the lighting performance.

Once the numbers of LEDs in series and parallel, respectively have been determined in this way, output voltage is determined according to the number of LEDs in series while output current is determined according to the number of LEDs in parallel. If the type of the final output power has been determined, it is now possible to determine operation topology. The final decision on the circuit of operation topology for realizing the output power should be made according to the types of the voltage and current to be applied to the terminal LED light source. Most of the LED operation circuits currently used for lighting adopt the method of square wave PWM regulation. This method can minimize the fluctuation range of light output and operation current and is advantageous for embodying such a constant-current circuit as shown in Fig. 2.

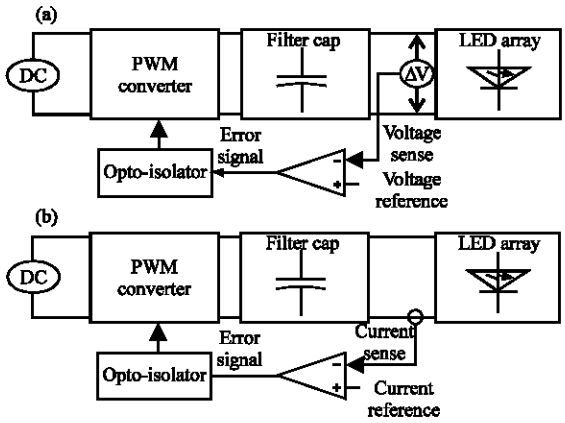

Fig. 1: LED driver using DC source; a) DC voltage to DC voltage type and b) DC voltage to DC current type

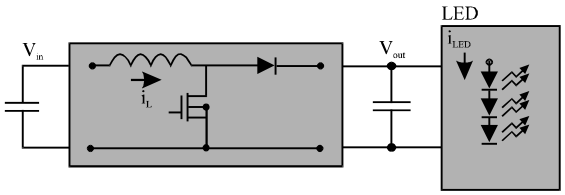

Fig. 2: Normal LED driver using the PWM control

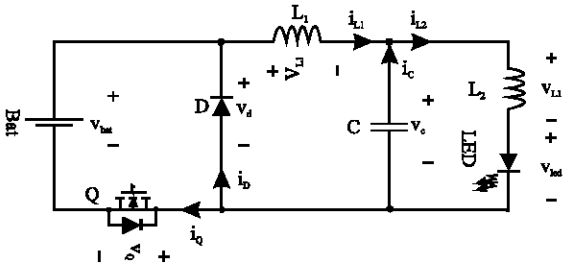

Fig. 3: Proposed soft switching buck converter

Secondary resonance: In general, a resonance circuit involves the sinusoidal current of an inductor and the sinusoidal voltage of a condenser. In such a primary resonance circuit, it is very difficult for sinusoidal voltage to be generated across any load that has the characteristics of voltage clamp such as an LED or a battery (Kong *et al*., 2004; Kwak *et al*., 2009; Yahaya *et al*., 2009).

For this reason, the present research configured a secondary resonance circuit, successfully in which an inductor was serially connected to the primary resonance circuit's load which maintained proper voltage. Figure 3 shows the DC/DC converter that has the new secondary resonance circuit and is capable of soft switching.

The basic topology of the proposed converter is a non-insulated buck converter. This topology consists of a primary resonance circuit involving L_1-C and a secondary resonance circuit involving L_2-C and the switch was connected to ground for Gate-Amp output. This circuit is characteristic in that secondary resonance is enabled by adding an inductor serially connected to LED.

The diode in Fig. 3 is a protection circuit that plays the role of a free-wheeling diode which is used for the converters that do not involve resonance such as a common buck converter.

The operation modes of the proposed circuit can be divided into 6 general modes and the interpretation of each operation mode is as follows.

Mode 1: As shown in Fig. 4, this mode begins at the moment the switch (Q) is turned ON when the currents of all the elements are 0 and the voltage of the

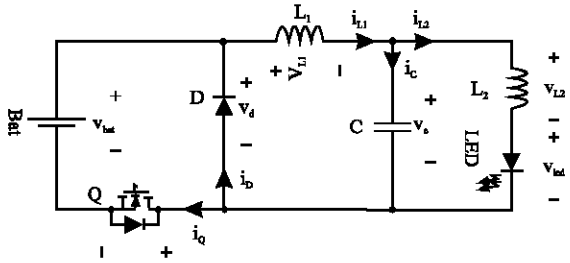

Fig. 4: Equivalence circuit of operation Mode 1

resonant condenser is the initial voltage $v_C(0)$. Resonance is achieved by L_1-C and the switch current (i_Q) is given by Eq. 1:

$$i_{L1} = \frac{(V_{bat}-v_c(0))}{Z_{r1}}\sin(\omega_{r1}t) + i(0)\cos(\omega_{r1}t) \quad (1)$$

From Eq. 1, the voltage of resonant C is as follows:

$$v_C(t) = V_{bat}-(V_{bat}-v_C(0))\cos(\omega_{r1}t)+i_{L1}(0)Z_{r1}\sin(\omega_{r1}t)$$

$$i_{L1}(T_2) = i_{L1}(t_1),\ V_C(T_2) = v_C(t_1) \quad (2)$$

$$Z_0 = \sqrt{\frac{L_1}{C}}: \text{Character impedence}$$

$$\omega_{r1} = \frac{1}{\sqrt{L_1 C}}: \text{Resonance impedance}$$

Therefore, as shown the switch current at the moment the switch Q is turned ON is 0 by Eq. 1, achieving ZCS:

$$i_Q(0) = 0 \quad (3)$$

This mode ends at the moment the condenser voltage (V_c) becomes equal to the threshold voltage of LED.

Mode 2: As shown in Fig. 5, at the moment when the resonant condenser C voltage becomes higher than the threshold voltage of LED, secondary resonance by L_1-C-L is achieved as current is generated in the inductor serially connected to LED.

The inductor L_2 current and the condenser C current in this mode are given by Eq. 4 and 5:

$$i_{L2} = \left(\frac{L_{r1}I_{L1}(T_2)}{L_{r1}+L_{r2}} + \frac{V_{bat}-V_{ZENER}}{L_{r1}+L_{r2}}t - \left(\frac{L_{r1}I_{L1}(T_2)}{L_{r1}+L_{r2}}\right)\cos(\omega_{r2}t)+ \left(\frac{\sqrt{L_{r1}}\sqrt{C_r}\,((V_C(T_2)-V_{ZENER})L_{r1}+(V_C(T_2)-V_{bmt})L_{r2})}{\sqrt{L_{r2}}\sqrt{L_{r1}+L_{r2}}\,(L_{r1}+L_{r2})}\right)\sin(\omega_{r2}t) \quad (4)$$

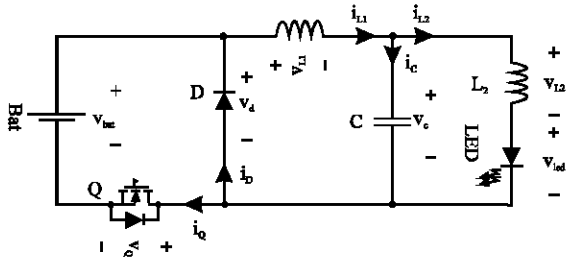

Fig. 5: Equivalence circuit of operation Mode 2

$$i_C = -\left(\frac{\sqrt{C_r}\,((V_C(T_2)-V_{ZENER})L_{r1}+(V_{bat}-V_C(T_2)L_{r2})}{\sqrt{L_{r1}}\sqrt{L_{r2}}\sqrt{L_{r1}+L_{r2}}}\right)\sin(\omega_{r2}t)+ I_{L1}(T_2)\cos(\omega_{r2}t) \quad (5)$$

From Eq. 4 and 5, the inductor L_1 current and the condenser C voltage are as follows:

$$i_{L1}(t) = i_{L2}-i_C \quad (6)$$

$$V_c(t) = V_c(T_2)-V_{ZENER}+V_{bat}- \left(\frac{(V_C(T_2)-V_{ZENER})L_{r1}+(V_{bat}-V_C(T_2))}{L_{r1}+L_{r2}}\right)\cos(\omega_{r2}t)+ I_{L1}(T_2)Z_{r2}\sin(\omega_{r2}t) \quad (7)$$

$$Z_{r2} = \sqrt{\frac{L_1 L_2}{(L_1+L_2)C}}: \text{Character impedence}$$

$$\omega_{r2} = \sqrt{\frac{L_1+L_2}{L_1 L_2 C}}: \text{resonnance frequence}$$

This mode ends at the moment the inductor L_1 current becomes 0.

Mode 3: As shown in Fig. 6, the inductor L_1 current is negative in this mode while the current is generated by the switch Q through the diode. Therefore, turning off the switch (Q) in this mode results in ZVS operation.

The inductor L_2 current and the condenser C voltage in this mode are given by Eq. 8 and 9:

$$i_{L2} = \frac{L_{r1}L_{L1}(T_2)}{L_{r1}+L_{r2}} + \frac{V_{bat}-V_{ZENER}}{L_{r1}+L_{r2}}t - \left(\frac{L_{r1}L_{L1}(T_2)}{L_{r1}+L_{r2}}\right)\cos(\omega_{r2}t)+ \left(\frac{\sqrt{L_{r1}}\sqrt{C_r}\,((V_C(T_2)-V_{ZENER})L_{r1}+(V_C(T_2)-V_{bat})L_{r2})}{\sqrt{L_{r2}}\sqrt{L_{r1}+L_{r2}}\,(L_{r1}+L_{r2})}\right)\sin(\omega_{r2}t) \quad (8)$$

$$i_C = -\left(\frac{\sqrt{C_r}\,((V_C(T_2)-V_{ZENER})L_{r1}+(V_{bat}-V_C((T_2))L_{r2})}{L_{r1}+L_{r2}}\right)\sin(\omega_{r2}t)+ I_{L1}(T_2)\cos(\omega_{r2}t) \quad (9)$$

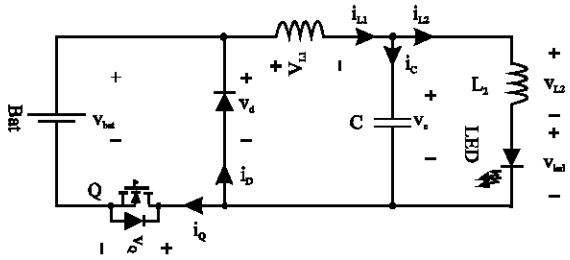

Fig. 6: Equivalence circuit of operation Mode 3

From Eq. 8 and 9, the inductor L_1 current and the condenser C voltage are as follows:

$$i_{L1}(t) = i_{L2} - i_C \tag{10}$$

$$v_C(t) = V_C(T_2) - V_{ZENER} + V_{bat} - \left(\frac{(V_C(T_2) - V_{ZENER})L_{r1} + (V_{bat} - V_C(T_2))}{L_{r1} + L_{r2}}\right)\cos(\omega_{r2}t) + I_{L1}(T_2)Z_{r2}\sin(\omega_{r2}t)$$

$$i_{L1}(T_4) = i_{L1}(t_3), V_C(t_4) = v_C(t_3) \tag{11}$$

This mode ends at the moment the inductor L_1 current becomes 0.

Mode 4: As shown in Fig. 7, the energy of the inductor L_2 is transferred to the condenser in this mode while a resonance circuit is formed involving the inductor L_2 and the condenser. The inductor current iL_2 sand the condenser voltage v_C are as follows:

$$i_{L2} = \frac{V_C(T_1) - V_{ZENER})}{Z_{r3}}\sin(\omega_{r3}t) + I_{L1}(T_4)\cos(\omega_{r3}t) \tag{12}$$

$$v_C(t) = V_{ZENER} - (V_C(T_2) - V_{ZENER})\cos(\omega_{r3}t) + I_{L1}(T_4)Z_{r3}\sin(\omega_{r3}t) \tag{13}$$

$$i_{L1}(T_5) = i_{L1}(t_4), i_{L2}(T_5) = i_{L2}(t_4),\ V_C(T_5) = v_C(t_4)$$

$$Z_{r3} = \sqrt{\frac{L_2}{C}} : \text{Character impedence}$$

$$\omega_{r3} = \sqrt{\frac{1}{L_2 C}} : \text{Resonance frequency}$$

This mode ends at the moment the condenser voltage becomes 0.

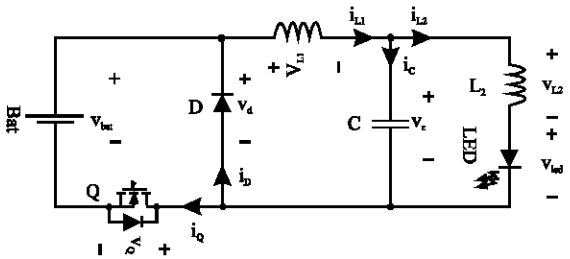

Fig. 7: Equivalence circuit of operation Mode 4

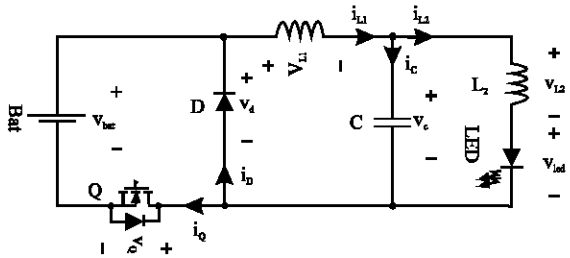

Fig. 8: Equivalence circuit of operation Mode 5

Mode 5: As shown in Fig. 8, the condenser voltage becomes negative by the energy transferred from the inductor L_2 in this mode.

The negative condenser voltage causes the formation of a current loop by the diode D and the inductor L_1. The inductor current i_{L1}, the condenser current, the inductor current i_{L2} and the condenser voltage v_C are as follows:

$$i_{L1} = \left(\frac{L_{r1}I_{L1}(T_5) + L_{r2}I_{L2}(T_5)}{L_{r1} + L_{r2}} - \frac{V_{ZENER}}{L_{r1} + L_{r2}}t + \left(I_{L1}(T_5) - \frac{L_{r1}I_{L1}(T_5) + L_{r2}I_{L2}(T_5)}{L_{r1} + L_{r2}}\right)\cos(\omega_{r2}t)\right) + \left(\frac{\sqrt{L_{r2}C_r}((V_{ZENER} - V_C(T_2))L_{r1} - V_C(T_2))L_{r2})}{\sqrt{L_{r1}}\sqrt{L_{r1} + L_{r2}}(L_{r1} + L_{r2})}\right)\sin(\omega_{r2}t) \tag{14}$$

$$i_C = -\left(\frac{\sqrt{C_r}((V_{ZENER} - V_C(T_5))L_{r1} - V_C(T_2)L_{r2})}{\sqrt{L_{r1}}\sqrt{L_{r2}}\sqrt{L_{r1} + L_{r2}}}\right)\sin(\omega_{r2}t) - (I_{L1}(T_5) - I_{L2}(T_5))\cos(\omega_{r2}t) \tag{15}$$

$$i_{L2}(t) = i_{L1}(t) + i_C(t) \tag{16}$$

$$V_C(t) = \frac{V_{ZENER}L_{r1}}{L_{r1} + L_{r2}} - \left(\frac{V_{ZENER} - V_C(T_5)L_{r1} - V_C(T_5)L_{r2}}{L_{r1} + L_{r2}}\right)\cos(\omega_{r2}t) + (I_{L1}(T_5) - I_{L2}(T_5))Z_{r2}\sin(\omega_{r2}t) \tag{17}$$

$$I_{L1}(T_6) = i_{L1}(t_5), V_C(T_5) = v_C(t_5)$$

This mode ends at the moment the inductor current iL_2 becomes 0.

Mode 6: As shown in Fig. 9, the energy of the inductor L_1 is transferred to the condenser in this mode. The inductor current i_{L1} and the condenser voltage v_C are as follows:

$$i_{L1} = -\frac{V_C(T_6)}{Z_{r1}}\sin(\omega_{r1}t)+I_{L1}(T_6)\cos(\omega_{r1}t) \quad (18)$$

$$v_C(t) = V_C(T_6)\cos(\omega_{r1}t)+I_{L1}(T_6)Z_{r1}\sin(\omega_{r1}t) \quad (19)$$

This mode ends at the moment the diode current becomes 0. Figure 10 presents the voltage-current operation waveform of the proposed converter according to the operation modes. The figure shows that ZCS and ZVS were achieved when the switch was turned on and off, respectively. Mode 6 corresponds to reactive power as shown in figure and it is desirable to eliminate it by selecting proper condenser capacity at the time of designing a high efficiency power conversion circuit.

Simulation circuit of converter: Figure 11 shows the simulation circuit diagram for the suitability verification and designing of the proposed converter. The simulation circuit allows the setting of reference current to obtain

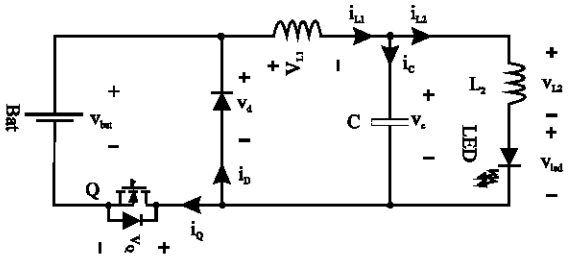

Fig. 9: Equivalence circuit of operation Mode 6

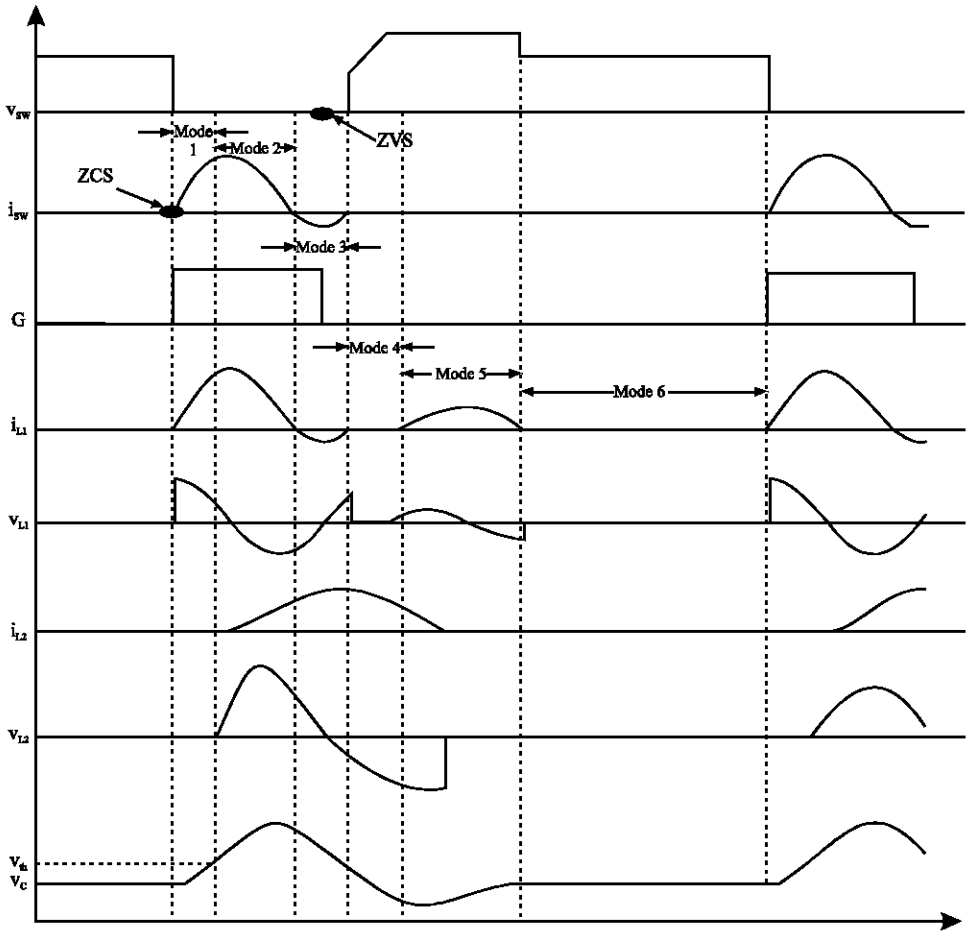

Fig. 10: Waveform of converter

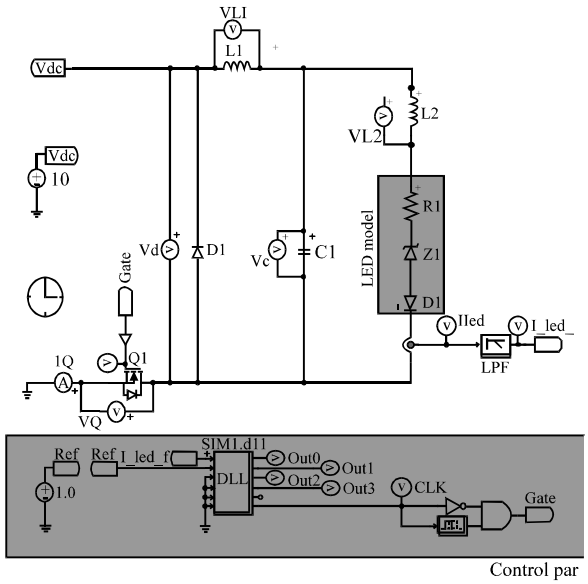

Fig. 11: Simulation circuit of converter

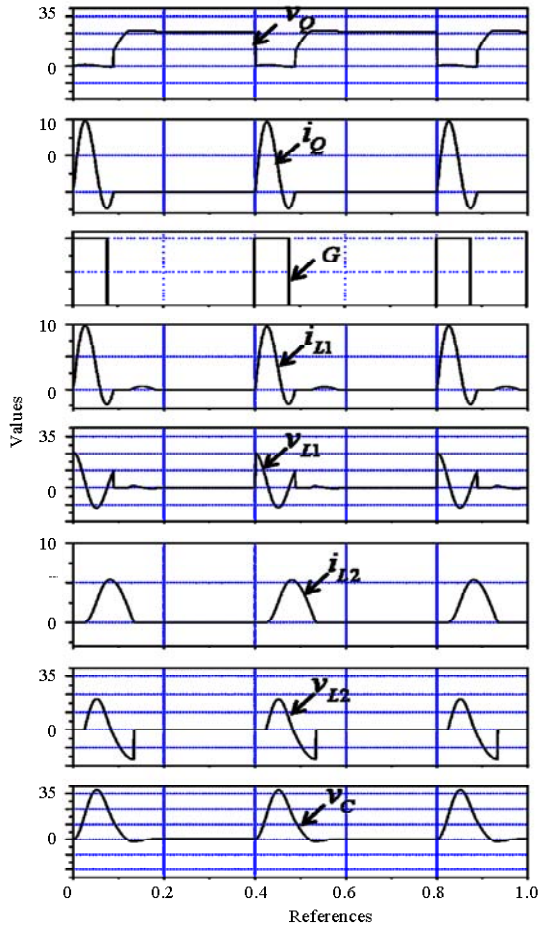

Fig. 12: Starting character of converter according to reference

Table 1: Main parameter of DC/DC converter

Parameters	No. of firms
Primary resonance inductor L1	3 u
Secondary resonance inductor L2	100 u
Resonance condenser C	1 uF

resulting constant current output. Figure 12 shows the result of simulation for examining the operation characteristics of the proposed secondary resonance circuit according to output.

The V_Q and I_Q in Fig. 12 represents the voltage and current of the switch. The G in the lower part of the figure shows the magnified waveform obtained from Gate-Amp output that correspond to the turning on and off of the switch.

In order to confirm the characteristics of the outputs obtained by resonance, definitions were made of the output waveform of the Voltage (V_{L1}) and current (I_{L1}) of the inductor where primary resonance occurred; as well as of the output waveform of the Voltage (V_{L2}) and current (I_{L2}) that indicated secondary resonance and also of resonance capacitor (Vc).

This figure demonstrates that ZVS was achieved when the switch was turned off and ZCS when turned on.

RESULTS AND DISCUSSION

Figure 13 shows the soft switching LED operation drive to which the proposed secondary resonance was applied as well as batteries and LED lamps.

The operation drive and the control chip used TMS320F028 to operate 360 W LEDs, charging batteries utilizing sunlight. Li-ion batteries (model name: SP24- 26F-52) were used whose operation voltage, rated current and capacity were 21-28 V, 15 A and 52 Ah, respectively.

The configuration of a total of 96 LED involved 6 serial and 16 parallel connections. The design involving 6 serial circuits resulted in an LED operation voltage of 18 V (about 86% of the minimum operation voltage of the battery) thus enabling LED operation only by buck converter action.

A characteristic of this topology is the insertion of inductor at the front-end of the switching element, condenser and load of a current-type resonant buck converter to achieve secondary resonance. That is to enable soft switching, this structure has an inductor serially connected to each of such loads as LEDs or batteries that maintain proper voltage in the primary resonance circuit.

Figure 14a and b show switch voltage, switch current, inductor current, resonance condenser voltage

Fig. 13: Prototype circuit board; a) operation drive; b) battery system and c) 96W LED lamp

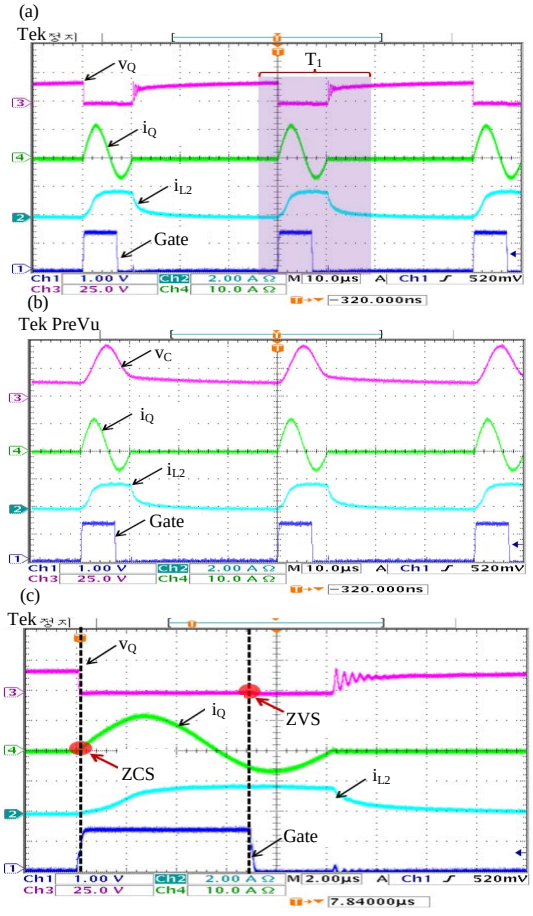

Fig. 14: a-c) Waveform of DC/DC converter at LED load

and gate signal during LED lamp operation at 25 kHz. In Fig. 14c, the waveform of Fig. 14a was magnified to confirm soft switching.

As shown in Fig. 14a, ZCS was achieved when the switch was turned on and ZVS when turned off as current

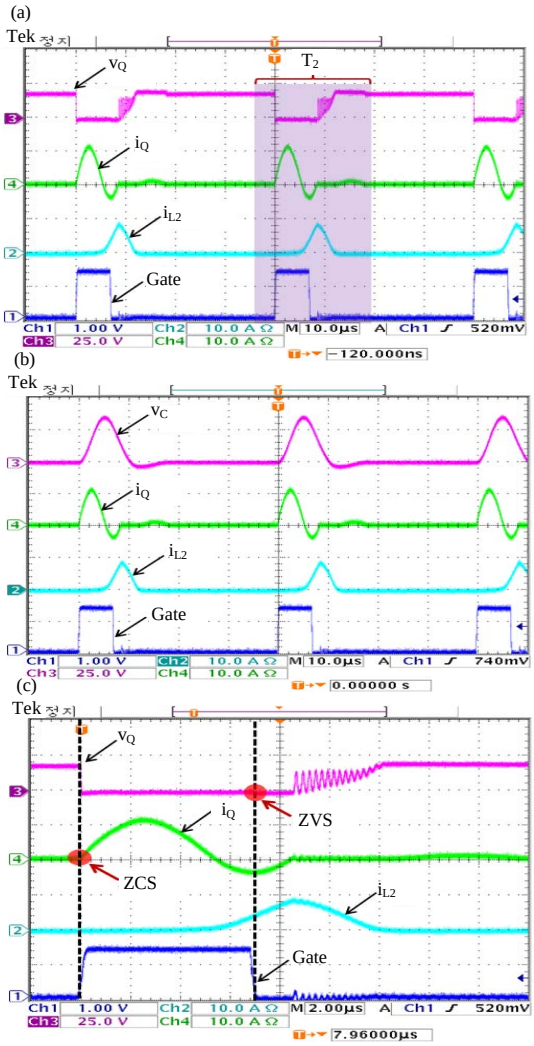

Fig. 15: a, b) Waveform of DC/DC converter at battery load

was generated at the diode inside the switch. And as shown in Fig. 14b, charged resonance condenser voltage was same as LED threshold voltage when the switch was turned off, indicating that secondary resonance inductor current was generated at the moment the switch was turned on.

Figure 15a, b show switch voltage, switch current, inductor current, resonance condenser voltage and gate signal while the battery was charged up to solar voltage at 25 kHz. In Fig. 15c, the waveform of Fig. 15a was magnified to confirm soft switching.

As shown in Fig. 15a, soft switching was achieved when the switch was turned on and off. And as shown in Fig. 15b, resonance condenser voltage was zero when the switch was turned off, indicating that secondary resonance inductor current was generated at the moment condenser voltage and battery voltage became same after

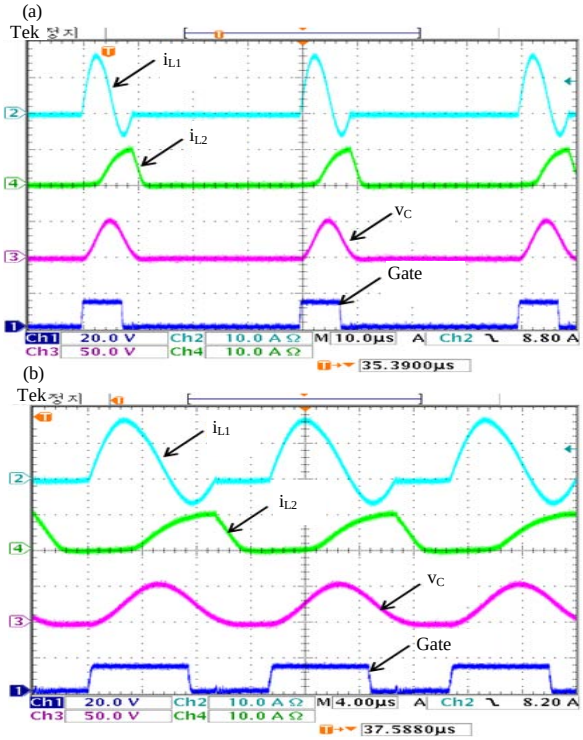

Fig. 16: Waveform of switching frequency; a) 25kHz and b) 70kHz

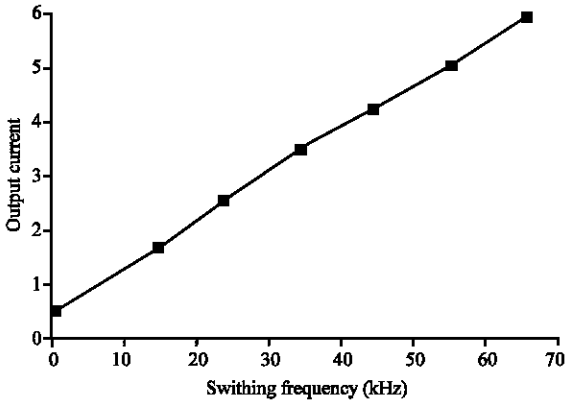

Fig. 17: The output current curve according to frequency changes

the switch was turned on. In order to control the proposed resonant DC/DC converter, switching frequency need to be controlled. Figure 16 shows resonance current, voltage and gate signal according to switching frequency. As shown in this figure, resonance was maintained regardless of changes in switching frequency, thereby enabling the switch to achieve soft switching regardless of switching frequency.

Figure 17 shows output current according to switching frequency. As shown in Fig. 17, output current

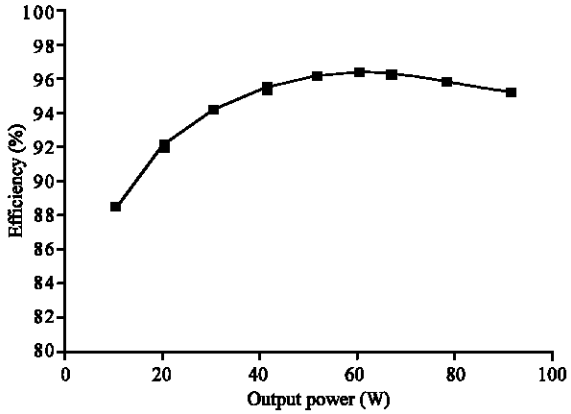

Fig. 18: The efficiency curve according to output

was almost proportional to switching frequency. As shown in this figure, a maximum efficiency of 96.2% was obtained when output power was 60 W.

CONCLUSION

This thesis proposed a new buck-type DC-DC converter topology for the LED operation drive and battery charge drive of an LED system for stand-alone solar security lights.

The proposed secondary resonant soft switching method could increase the efficiency of power converter by enabling soft switching both when the switch was turned on and when turned off.

When battery SOC was low, the proposed drive could achieve increase in number of sunless days by controling dimming through switching frequency control. In addition by designing an LED lamp that was suitable for battery operation voltage which involved a buck convert that enabled the designing of LED operation range, it was possible to achieve high efficiency of the whole system.

REFERENCES

Choi, J.B., K.W. Kim, Y.G. Jung and Y.C. Lim, 2009. A study on the modularization of LED driver for illumination using a fly-back converter. Trans. Korean Inst. Power Electron., 14: 504-513.

Kang, M.G., 2013. A comparison of DC-DC buck converter controller. J. Inst. Electron. Inf. Eng., 50: 281-285.

Kong, Y.S., E.S. Kim, S.C. Yang, J.M. Kim and B.C. Shin, 2004. Non-contact power supply using the series-parallel resonant converter. Trans. Korean Inst. Power Electron., 9: 405-412.

Kwak, D.K., S.H. Lee and D.Y. Jung, 2009. A new buck-boost dc/dc converter of high efficiency by soft switching technique. Proceedings of the 6th IEEE International Conference on Power Electronics and Motion Control (IPEMC 09), May 17-20, 2009, IEEE, Wuhan, China, ISBN:978-1-4244-3556-2, pp: 1295-1299.

Park, K.M., K.I. Lee, S.S. Hong, S.K. Han and C.W. Roh, 2009. New LED driver circuit to reduce voltage stress. Trans. Korean Inst. Power Electron., 14: 243-250.

Shin, D.S., Y.J. Jung, S.S. Hong, S.K. Han and B.J. Jang *et al*., 2010. A high efficiency LED driver circuit using LLC resonant converter. Trans. Korean Inst. Power Electron., 15: 35-42.

Yahaya, N.Z., K.M. Begam and M. Awan, 2009. Design and simulation of an improved soft-switched synchronous buck converter. Proceedings of the 3rd Asia International Conference on Modelling & Simulation (AMS'09), May 25-29, 2009, IEEE, Bali, Indonesia, ISBN:978-1-4244-4154-9, pp: 751-756.